DOI: 10.13009/EUCASS2023-324
Aerospace Europe Conference 2023 – 10TH EUCASS – 9TH CEAS

Thermal effects in optomechanical systems for space applications

Fatouma MAAMAR [1], Omar MERTAD[2], Abdeldjelil MANKOUR[3]*

[1,2,3] ASAL, Algerian Space Agency, Satellites development center, BP4065, Ibn Rochd USTO, Oran, POS 50 ILOT T12 Bir El Djir 31130, Oran, ALGERIA, fmaamar@cds.asal.fr ., Omertad@cds.asal.fr ., ajmankour@cds.asal.fr

Abstract

Optomechanical systems are often required to operate across a wide temperature range, which can significantly affect their performance. In this paper, we describe the impact of temperature changes on typical optomechanical systems and present our investigation into thermal stresses caused by continuous edge, six point, and face elastomeric bonds using both analytical methods and finite element models (FEM) software. We calculated analytical equations for the thermalized edge bond thickness, thermal stress, and the thermal optical path difference (OPD) where possible, and verified them through finite element solutions. The thermal OPD varies with temperature and can cause thermo-optic distortion, which can pose serious challenges for high-resolution optical systems. Our analysis shows that simple analytical solutions provide low estimation errors for thermal stresses and can be highly valuable for decision-makers and optical engineers during the development phases of space optomechanical systems.

Keywords: Bonded optic, Elastomer, Thermal stress, Thermo-optic coefficient, OPD

DOI: 10.13009/EUCASS2023-324

1. Introduction

The precision of opto-mechanical systems under a drop temperature require athermal mounting structures. High performances of lens mounting require integrated optomechanical analysis to predict optical performance. This requires that an analytical method and finite element analysis (FEA) bring out the relative importance of different lenses and material parameters. also, it gives some insight into different stress analyses in which the bonds might fail.

Several research studies were conducted in the field of athermal design, starting with a lens design provided by the optical designer, to create a structure, which the mount minimize thermo-elastic stresses and maintain the axial/radial alignment of a lens element. In addition, to minimize the axial and lateral stresses considerations, the mechanical designer called for an incredibly low distortion with the guidance of Daniel Vukoratovich [1] a sub-cell approach using elastomeric bond material, when the elastomeric mounting method adjusts the thickness of a bondline filling the gap between a lens and a cell [2]. The problem of athermal bonding thickness was first proposed by Bayar [3] used a simple equation using CTE (coefficient of thermal expansion) differences of the various materials in the lens mount to arrive at the optimum bond thickness. Another athermal bondline equation is the Muench [4-5] derived an equation using CTEs and Poisson's ratio. From Deluzio [6] derived an equation for an athermal bondline that accounts for the hydrostatic effect of the in-plane strains of the bond being essentially zero. The next equation published is Van Bezooijen [7] the required athermal radial thickness is given if the elastomer is constrained in radial and axial directions. An intermediate approximation between the upper and lower limits of the required elastomer thickness which includes the bulging of the elastomer as the temperature changes is given by Monti's aspect ratio approximation [8-9].

Actually, several simple analytical equations were discussed, including thermal stress, radial stress and lens diffraction limited by calculated optical path difference (OPD) [10]. This study has listed the material properties for glasses, metal, and adhesive. While one usually thermal stress with the stresses that arise from drop temperature service condition on materials with dissimilar thermal expansion coefficient, such this difference about coefficient reduces thermal stress between the lens and mount, and can cause low stresses in the lens. Additionally, for radial stress in lens assembly occur because of the mismatch in coefficients of thermal expansion of lens, bonding layer and barrel. The radial stress [9] depends greatly on the properties mechanical of all assembly material and temperature change. Another way in which the mechanical stress influences the optical performance is directly through deformation of optical surfaces. Axial deflection of optical surface can contribute to Wavefront error. Wavefront errors are often given in the form of an optical path difference (OPD) [11]. Sparks and Cottis [12] provided equations for the minimum thickness required to reduce the OPD from pressure -induced distortion to an eighth the wavelength. A maximum OPD of an eighth the wavelength is below the diffraction limit for an optical component (Rayleigh criteria) [13-15].
After a brief discussion on the existing research basics of the effect athermal bond thickness and different stress analysis on lens, this paper will provide an overview of the finite element analysis by evaluated design between the parametric analytical analysis and the FEA [16] to achieve an optimal design for mounting a lens to consider reduction the Gap and radial stress in the lens.

2. Structural analysis

Many optomechanical system are attached to their mounts with a thin adhesive layer. Furthermore, a six number of contact glue pads mount to be perfectly kinematic with an adhesive bond. The bond area required to handle the environment loads can be large enough to require an analysis of the bond layer effects on the performance optic. Bond layers cause distortion of optics due to the following:

- Bond layer relative growth due to a mismatch of CTE
- Bond layer contraction during curing
- Bond layer growth due to moisture absorption

A simple technique for mounting lenses is illustrated schematically in Fig.1. shows are typical design for a lens fixed in barrel by assembly structural using epoxy adhesive bonding. EA 2216 epoxy made by 3M has been used for this purpose and is representative of that class of elastomer. Its outgassing characteristics are sufficiently low for it to be used with great success in space applications. All the mechanical properties materials of barrel, lenses and adhesives are presented in Table 1. Unfortunately, values for important

DOI: 10.13009/EUCASS2023-324

properties such as Poisson's, Young's Modulus and thermal expansion coefficient (CTE) are generally available for these materials.

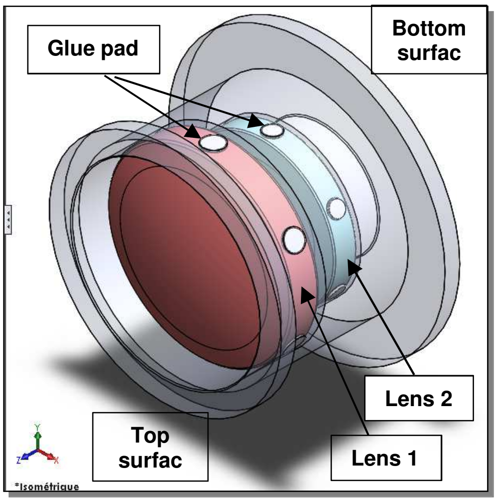

Fig. 1. A lens mounting configuration

Table 1. Parameters defining the materials

Part	Barrel	Glue	Lens1	Lens2
Material	Aluminium	Epoxy	N-SF11	NK-5
Young's Modulus E(MPa)	69000	(4700÷70) for (-40°C÷20°C)	92000	71000
Poisson's Ratio ν	0.2	0.39	0.257	0.224
Coefficient of Thermal Expansion CTE.10^{-6}(/K)	0.23	102	8.5	8.2
Thermal Conductivity λ (W/m.k)	184	-	-	0.81
Mass Density ρ (Kg/m^3)	2801	1260	3220	2590

The detailed view in Figure. 1 illustrates one method for securing the lens in position and containing the elastomer during the curing process. The barrel, constructed from Aluminum and coated with a mold release agent, is removed once the curing is complete. The elastomer is typically injected using a hypodermic syringe through access holes that are radially oriented in the mount until the area surrounding the lens is filled, as shown in Figure 2.

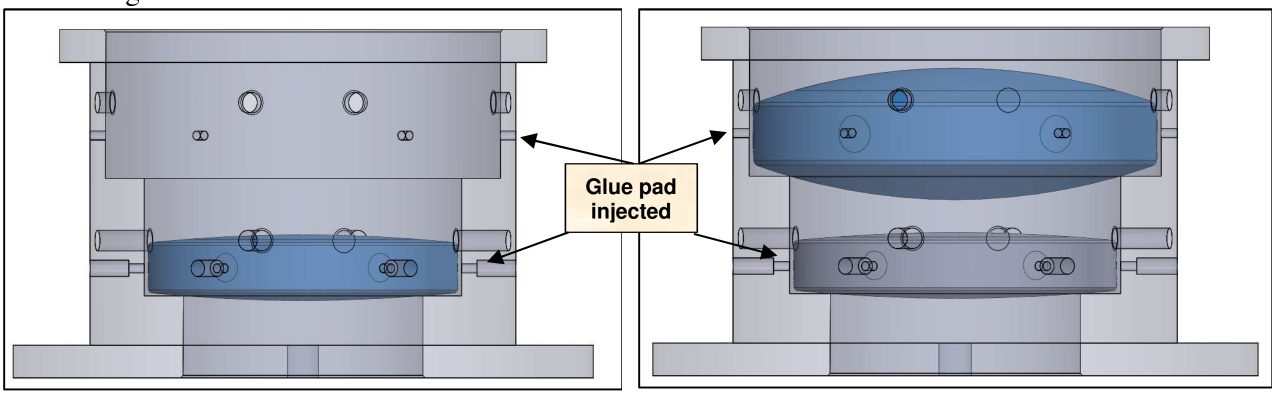

Fig. 2. Holes the lens mount

To ensure optimal mitigation of the effects of thermal expansion, it is recommended to undersize the bore. This will allow the elastomer layer to achieve the desired thickness, denoted as h_r, which in turn results in an athermal assembly in the radial direction to a first order approximation. Such an approach minimizes stress buildup within the optomechanical components, which typically arises from differential radial expansion or contraction of the lens, barrel, and glue pad under varying temperatures. The Bayar equation can be used to

DOI: 10.13009/EUCASS2023-324

calculate the ideal athermal radial elastomer thickness, assuming the elastomer is in a zero-stress condition, and considering the radial change in clearance between the lens and barrel width;

$$h_{r,Bayar} = r_{optic}\frac{\propto_m - \propto_{optic}}{\propto_G - \propto_m} \tag{1}$$

Where:

r_{optic}	The lens ratio in mm
α_m	The thermal expansion coefficient of the barrel (ppm/°C)
α_{optic}	The thermal expansion coefficient of the lens (ppm/°C)
α_G	The thermal expansion coefficient of the glue pad (ppm/°C)

The Bayar equation neglects the effects of Poison's ratio and confinement of the elastomer. Another equation for $h_r$that does include the effect of Poison's ratio is the so-called "Muench equation" where the elastomer's bulk CTE is used:

$$h_{r,Muench} = r_{optic}\frac{(1-\nu_m).\left(\alpha_m - \alpha_{optic}\right)}{\alpha_G - \alpha_m + \nu_G.\left(\alpha_G - \alpha_{optic}\right)} \tag{2}$$

Deluzio presents an equation to athermal size adhesive bonds expressed in equation (3)

$$h_{r,Deluzio} = r_{optic}\frac{1-\nu_G}{1+\nu_G}.\left[\frac{\alpha_m - \alpha_{optic}}{\left(\alpha_G - \alpha_{optic}\right) - \frac{(7-6\nu_G).\left(\alpha_m - \alpha_{optic}\right)}{4.(1+\nu_G)}}\right] \tag{3}$$

Van Bezooijen define the upper and lower limits of the required elastomer thickness in radial and axial direction. In the axial direction, the elastomer is constrained to the surface of lens and barrel. The optimum athermal elastomer thickness h_r is:

$$h_{r,VB} = r_{optic}\frac{\alpha_m - \alpha_{optic}}{\alpha_G - \alpha_m + \frac{2\nu_G}{1-\nu_G}\left(\alpha_G - \frac{\alpha_{optic}+\alpha_m}{2}\right)} \tag{4}$$

With ν_G is the Poisson's ratio of the elastomer

Monti's aspect ratio approximation equation includes the bulging of the elastomer as the temperature changes. The aspect ratio approximation is closest to results from finite-element analysis. The optimum athermal radial thickness is given by:

$$h_{r,MAR} = \frac{-b+\sqrt{b^2-4ac}}{2a} \tag{5}$$

DOI: 10.13009/EUCASS2023-324

$$a = \frac{-\nu_G}{L}\left(\alpha_G - \frac{\alpha_{optic} + \alpha_m}{2}\right) \qquad c = -r_{optic}(1 - \nu_G)(\alpha_m - \alpha_{optic})$$

$$b = (1 - \nu_G)(\alpha_G - \alpha_m) + 2\nu_G\left(\alpha_G - \frac{\alpha_{optic} + \alpha_m}{2}\right)$$

Where L is the length of elastomer

are listed in Table.2

Table 2. Athermal bond thickness comparison

Equation	Bayar	Muench	Deluzio	Van Bezooijen	Monti's
Lens 1; N-SF11, 50 mm diameter, 74.78 mm Radius of curvature, 16 mm Center thickness					
h_r (mm)	2.0315	0.9229	0.9166	0.9229	0.9088
Lens 2; N-K5, 40mm diameter, 207.93 mm Radius of curvature, 8 mm Center thickness					
h_r (mm)	1.5663	0.7109	0.7063	0.7110	0.6945

From Table 2, the inaccuracy of equation Bayar is offset by the low stiffness of the elastomers typically used to bond the lens into the barrel. The radial thickness given by the Bayar equation is greater than that given by equations 2 through 5, which provides additional radial compliance to reduce thermal stress. However, approaches of Muench, Deluzio, Van Bezooijen and Monti's equations track very closely and can be used for most athermal optimum bundling calculations.

- The bonding surface should be as dry as possible prior to bonding
- Optics made from brittle materials need polished surface at the bonding to maximize strength
- Keep bonds away from the surface interfaces of the optic

3. Thermal analysis

In optomechanical design, the correct attachment of the six-point edge glue pad of lenses to barrel structures is crucial. Opto-elasticity due to thermal stresses and radial stress at the optic/bond interface is a major concern. Thermal stress arises due to differences in the coefficient of thermal expansion (CTE) between the glue pad and lenses when the adhesive is attached to the surface of the lens. Typically, the adhesive is made of an epoxy with a high CTE material. The CTE values for the adhesive, lenses, and barrel have a qualitative relationship where $\alpha_G \gg \alpha_m > \alpha_{optic}$. Most epoxies have low elastic moduli, but are nearly incompressible. Young's modulus increases with decreasing temperature [17], and Poisson's ratio is close to 0.4. The mismatch of thermal expansion coefficients, in conjunction with the low compressibility of the epoxy, can cause high stresses in the epoxy layer. The thermal stress depends greatly on the bond thickness, and the thickness can be adjusted to minimize or even eliminate the stress. The thermal stress in the optic can be given approximately by [18]:

DOI: 10.13009/EUCASS2023-324

$$\sigma_T = -E_G.\varepsilon.\left[\frac{1+\frac{\nu_G}{1-2\nu_G}}{1+\nu_G}\right] \tag{6}$$

$$\varepsilon = \frac{\Delta h}{h_e+\Delta h}\left\{\alpha_G - \frac{2\nu_G}{1-\nu_G}\left[\frac{(\alpha_m-\alpha_{optic})}{2} - \alpha_G\right]\right\}\Delta T$$

Where; $E_G$is the elastic modulus of the glue pad, Δh_e is the variation in glue pad thickness, and ΔT is temperature difference.

Table 3. Thermal stresses for each element lens in MPa for different temperatures

	Temperature (°C)						
	20	0	-5	-10	-20	-25	-30
	Thermal stress (MPa)						
Lens 1	0	8.9593	12.5243	14.5585	26.0284	74.7434	155.180
Lens 2	0	8.9505	12.5110	14.5397	25.9964	74.7036	155.131

Bonding of the lenses mount hardware occurred at room temperature (about 20°C), while the service temperature was as low as seven different values (20, 0°C, -5°C, -10°C, -20°C, -25°C and -30°C). From Table.3. Further weak in temperature will increase the thermal stress, which is detailed in the following points:

- The thermal stress increases from 20°C to -30°C for both lenses
- All constraints are zero in the vicinity of the ambient temperature for both lenses
- All constraints are almost equal for both lenses, which explained the presence of a parameter's mechanicals temperature gradient, the thermal stress is proportional to the thermal distortion coefficient for space applications. Indeed, small difference in CTE the lenses, we found these results.

In summary, our analysis suggests that the lens is held in place by the glue pad, and slippage occurs between the two surfaces when there is a change in temperature. This slippage limits the thermal stress to a negligible level that is unlikely to cause issues, but it is still advisable to examine for any possible radial stress optic effects. However, to determine the optimal solution, further investigations are needed to calculate the radial stress at the optic/bond interface when there is a sudden temperature drop. This drop may lead to a radial force exerted on the lens rim, resulting in radial compression and generating radial stress. The degree of approximation considered only accounts for thermal stress and radial stress, which can adversely affect the optic's performance if they reach a significant level. In severe cases, these stresses may cause the lens to fail or the mount to deform. Therefore, a more thorough investigation is required to arrive at an optimal solution.

Radial stress is induced in the lens when the temperature is lowered enough for the barrel to come into contact. The radial stress from the temperature change ΔT at the lens/bond interface as a function of bonding thickness is given by [19]:

$$\sigma_r = \frac{E_G.\Delta T}{4.(1-2.\nu_G).(1+\nu_G)}\left\{(\alpha_m-\alpha_{optic})\left[\frac{2(5-4\nu_G)r_m^2}{r_m^2-r_{optic}^2} - \frac{1}{ln\frac{r_m}{r_{optic}}}\right] - 4(1+\nu_G)(\alpha_G-\alpha_{optic}\right\} \tag{7}$$

Where;

r_{optic} is radius of lens,

$r_m = r_{optic} + h$ with h is the radial wall thickness of the barrel,

DOI: 10.13009/EUCASS2023-324

Table.4, gives the radial stress foe each element 'lens' in MPa for different temperatures.

Table 4. Radial stress for each element lens in MPa for different temperatures

	Temperature (°C)						
	20	0	-5	-10	-20	-25	-30
	Radial stress (MPa)						
Lens 1	0	25.677	35.754	42.128	73.712	218.742	458.811
Lens 2	0	25.692	35.776	42.158	73.764	218.810	458.895

We can see from Table.4, the distribution of the radial stress depending on the temperature drop, that are the most important at the cantilever level, which is coherent. Further weak in temperature will increase the radial stress, which is detailed in the following points:

- The highest radial stress is obtained in lens 2, which had great parameter dimensional as diameter and parameter property thermal materials as coefficient of thermal expansion at -30°C temperature,
- The radial stress increases from 20°C to -30°C for both lenses,
- All constraints are zero in the vicinity of the ambient temperature for both lenses,
- The less stress is obtained in lens 1 at 0°C temperature a value of 25.677MPa, after the value nullity in the vicinity of the ambient temperature,
- All constraints are positive for both lenses, which explained the uniformity of the coefficient of thermal expansion for space applications.

Indeed, the results obtained for both lenses are acceptable stress, and there is no risk of structural failure. The allowable radial stress for lens materials is set by the distortion or diffraction tolerance of the optical surface. Lenses materials are perfectly elastic up until failure, so the allowable stress is the failure stress associated with some probability of failure at a given lifetime. Whereas, it would be desirable to check for optical effects by using optical path difference and compared par admissible optic.

4. Optical system performance analysis

In the process of lens assembly, it is crucial to consider not only thermo-elastic distortion but also the impact of temperature-induced changes in the index of refraction (thermo-optic effects) and stress-induced changes (stress-optic effects) on optical performance. Changes in the index of refraction due to temperature and stress can have a significant impact on optical performance. To accurately predict the performance, it is necessary to integrate these effects into the optical analysis by computing the net effect as an optical path difference (OPD).

In the case of assembling two lenses with different materials, the index of refraction (n) is a function of temperature (T), and as a result, the performance of a lens subjected to temperature changes can be affected by dn/dT effects. An optics program can import the optical path difference (OPD) to be applied to optical surfaces, which accounts for the thermo-optic-index change. The thermo-optic coefficient can be calculated using the following relationship [20]:

$$\frac{dn_{rel}}{dT} = \frac{n_{rel}^2 - 1}{2n_{rel}}\left(D_0 + 2D_1\Delta T + 3D_2\Delta T^2 + \frac{E_0 + 2E_1\Delta T}{\lambda^2 - \lambda_{TK}^2}\right) \tag{8}$$

$$n_{rel}^2 - 1 = \frac{B_1\lambda^2}{\lambda^2 - C_1} + \frac{B_2\lambda^2}{\lambda^2 - C_2} + \frac{B_3\lambda^2}{\lambda^2 - C_3}$$

DOI: 10.13009/EUCASS2023-324

Where

n, is the index of refraction

$(B_1, B_2, B_3, C_1, C_2, C_3)$, Constants of the Sellmeier dispersion formula

$(D_0, D_1, D_2, E_0, E_1, \lambda_{TK})$, Constants for the calculation of the temperature coefficients of refractive index dn/dT.

Table 5. Data constants for the calculation of the thermo-optic coefficient for each element lenses

Optical Glass	n_d	n_e	Constants of the dispersion formula					
			B_1	B_2	B_3	C_1	C_2	C_3
Lens 1	1.7847	1.7919	1.7375	$3.137e^{-1}$	1.8987	$1.318e^{-2}$	$6.230e^{-2}$	$1.552e^{+2}$
Lens 2	1.5225	1.5245	1.0852	$1.996e^{-1}$	$9.305e^{-1}$	$6.610e^{-3}$	$2.411e^{-2}$	$1.119e^{+2}$
			Constants for dn/dT					
			D_0	D_1	D_2	E_0	E_1	λ_{TK}
Lens 1	1.7847	1.7919	$-3.56e^{-6}$	$9.20e^{-9}$	$-2.10e^{-11}$	$9.65e^{-7}$	$1.11e^{-9}$	$2.94e^{-1}$
Lens 2	1.5225	1.5245	$-4.13e^{-7}$	$1.03e^{-8}$	$-3.40e^{-11}$	$4.73e^{-7}$	$5.19e^{-10}$	$2.13e^{-1}$

Table 5 provides the constant data for dispersion and refractive index of each lens element at 587.5618 nm wavelength (d-line) and 546.0740 nm wavelength (e-line). To create the thermo-optic model, the CTE is replaced by the thermo-optic coefficient (dn/dT), Poisson's ratio is set to zero, the shear modulus is defined as one, and the temperature distribution is used as the applied load. Furthermore, the thermo-optic model requires that the nodes on the front surface of the optical element are constrained to zero displacement, and the remaining nodes are constrained to zero displacement, except along the direction of the light path. After running the model, the displacement of the rear surface of the lens represents the OPD errors across the wave front. This analysis is based on the relationship:

$$OPD = \left[\frac{dn_{rel}}{dT}\right].h.\Delta T \tag{9}$$

Where h is thickness axial of the lens and ΔT is the temperature gradient from the center to a point on the edge of the lens. The CTE accounts for the change in OPD due to thickness changes, and the thermo-optic coefficient accounts for the change in the index of refraction. Table.6, gives the values of the thermo-optic coefficient and OPD for different temperature for each element lenses.

Table 6.Values of the thermo-optic coefficient (1/K) and OPD (m) for each element lenses
for different temperatures and different wavelength (nm)

Optical Glass	Temperature difference ΔT, with T_0=20°C, $\lambda_1 = 587.5618\,nm,\ \lambda_2 = 546.0740\,nm$

DOI: 10.13009/EUCASS2023-324

			20°C	0°C	-5°C	-10°C	-20°C	-25°C	-30°C
Lens 1	λ_1 (nm)	dn/dT (1/K)	$3.94e^{-7}$	$4.38e^{-7}$	$4.49e^{-7}$	$4.61e^{-7}$	$4.87e^{-6}$	$5e^{-6}$	$5.13e^{-6}$
		OPD(m)	0	$1.40e^{-7}$	$1.80e^{-7}$	$2.21e^{-7}$	$3.11e^{-7}$	$3.60e^{-7}$	$4.11e^{-7}$
	λ_2 (nm)	dn/dt (1/K)	$3.92e^{-7}$	$4.36e^{-7}$	$4.48e^{-7}$	$4.60e^{-7}$	$4.85e^{-6}$	$4.98e^{-6}$	$5.11e^{-6}$
		OPD(m)	0	$1.39e^{-7}$	$1.79e^{-7}$	$2.21e^{-7}$	$3.10e^{-7}$	$3.58e^{-7}$	$4.09e^{-7}$
Lens 2	λ_1 (nm)	dn/dT (1/K)	$3e^{-7}$	$6.30e^{-7}$	$7.22e^{-7}$	$8.17e^{-7}$	$1.02e^{-6}$	$1.13e^{-6}$	$1.24e^{-6}$
		OPD(m)	0	$1.01e^{-7}$	$1.44e^{-7}$	$1.96e^{-7}$	$3.26e^{-7}$	$4.05e^{-7}$	$4.94e^{-7}$
	λ_2 (nm)	dn/dT (1/K)	3e-7	$6.29e^{-7}$	$7.21e^{-7}$	8.16e-7	$1.02e^{-6}$	$1.12e^{-6}$	$1.23e^{-6}$
		OPD(m)	0	$1.01e^{-7}$	$1.44e^{-7}$	$1.96e^{-7}$	$3.26e^{-7}$	$4.05e^{-7}$	$4.94e^{-7}$

Upon analyzing Table.6, it is evident that the results align with the expected behavior, where the thermo-optic coefficient and optical path difference (OPD) are directly proportional to the wavelength of the optical system. It is important to note that any temperature variation will cause an increase in the optical parameters, as outlined below:

- The thermo-optic coefficient increases from 20°C to -30°C regardless of wavelength for both lenses,
- All value of optical path difference OPD are zero regardless of the wavelength in the vicinity of the ambient temperature,
- The highest OPD is obtained in lens 1, which has strong CTE compared to lens 2 at -30°C temperature,
- The OPD increase from 20° to -30°C regardless wavelength for both lenses
- The less value of OPD is obtained in lens 2, which had small thickness axial of the lens regardless temperature and wavelength.

Temperature is varied in two value of wavelength study; the design was optimum keeping Rayleigh criteria in view that considered to be perfect or diffraction limited, which is that OPD ≤ 8. However, when performing less distortion on the lens, the main interest is focused on determining the maximum OPD of the lens due to the thermal loads rather than verifying optimum bond thickness between the lens and barrel.

The maximum in the lenses path OPD on the reflected wavelength induced by thermal distortion of the lenses surface is given in Table.7.

Table 7. values of the maximum OPD (nm/cm) for each element lenses for different temperatures and different wavelength (nm)

Glasses	Temperature difference ΔT, with T_0=20°C, $\lambda_1 = 587.5618\ nm,\ \ \lambda_2 = 546.0740\ nm$						
	20°C	0°C	-5°C	-10°C	-20°C	-25°C	-30°C

DOI: 10.13009/EUCASS2023-324

Lens 1	λ_1	0	1.4	1.797	2.215	3.115	3.599	4.107
	λ_2	0	1.395	1.790	2.206	3.102	3.584	4.090
Lens 2	λ_1	0	1.0079	1.4431	1.9606	3.2600	4.0509	4.9417
	λ_2	0	1.0065	1.4412	1.9580	3.2556	4.0454	4.9351

We observe from Table above that the optical path difference OPD is well below the normal quarter wavelength tolerance for diffraction-limited systems for both lenses regardless variations the temperature and two values of the wavelength. This is again for a worst-case thermal effect. Thermal effect requires a modification for the value of the OPD. The optical path of the lens is required for evaluation of diffraction limited or less surface distortion. Even more to thermo-optic effects, but also there is the stress optic OPD limits the stress in the lens. Usually, the stress induced at the interface between the lens and mount is highly localized. To get these effects stress into the opto-mechanical analysis. Simple closed form analyses coupled with worst-case assumptions are desirable for design estimates. If this analysis indicates that there is sufficient performance margin, design is perfect. When analysis indicates insufficient margin, more accurate methods, such as finite-element analysis (FEA), are necessary before beginning the evaluate and validate the approach Analytical.

5. FEA Parametric Evaluation

Taking the lens assembly as the second research object by using finite element analysis (FEA) in this paper. There are often large differences in the estimated performance between FEA and approach analytical. The letter serves as a good check for preliminary FEA. Good agreement is usually defined as agreement between these results within about 10%. The acceptable design is guided by the FEA, although it may be necessary to iterate between the parametric analytical analysis and the FEA to achieve an optimal design.

The assembly size and material parameters are shows in Fig.3 and Table. 1. We used Solidworks for the computer aided design (CAD) and Ansys software for FEA. The base of main housing stand is fixed with six degrees of freedom (DOF) available for the used elements. The lens mounting is analyzed for the following loads conditions;

- Ambient temperature T=+20°C
- Thermal load; the structure is subjected to a temperature variation (20°C, 0°C, -5°C, -10°C, -20°C, -25°C and -30°C)
- The model bottom boundary is fixed in all directions according to Fig.1.
- The top surface is free in all directions according to Fig.1.

The adhesive pads were modelled using linear quadrilateral type and quadratic quadrilateral elements, when had same refined mesh on bond lens in order to achieve better accuracy, as shown in Fig.4 and 5. Obtained the radial stress in the lenses under different temperature. The temperature load is applied to the established finite element model, and the radial stress coupling two analysis who understood analytical (Eq.7) and FEA are performed by the direct method to obtain the stress distribution curves of each lenses through the results, as shown in Fig.6.

DOI: 10.13009/EUCASS2023-324

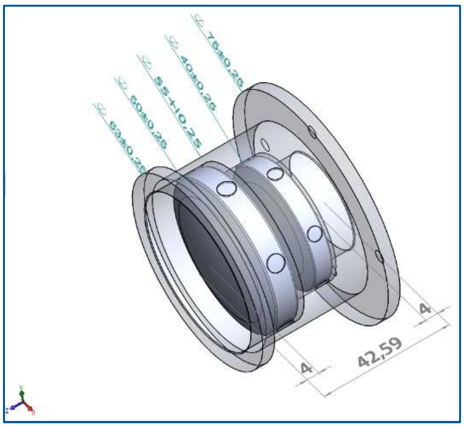

Fig. 3. Assembly sizing

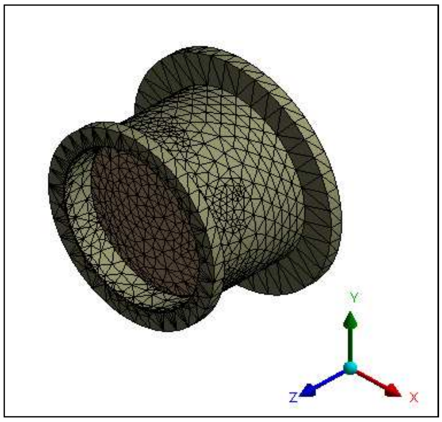

Fig. 4. Default mesh for assembly monitoring

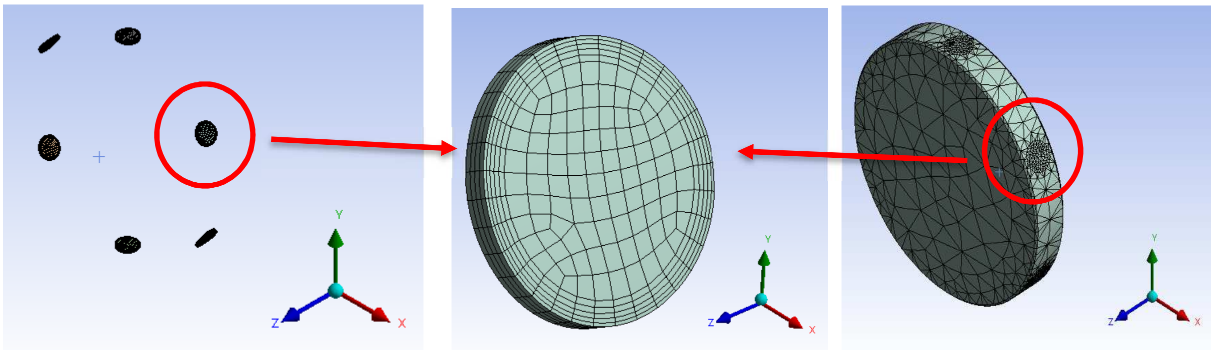

Fig. 5. Refined mesh for Glue Pads and lens

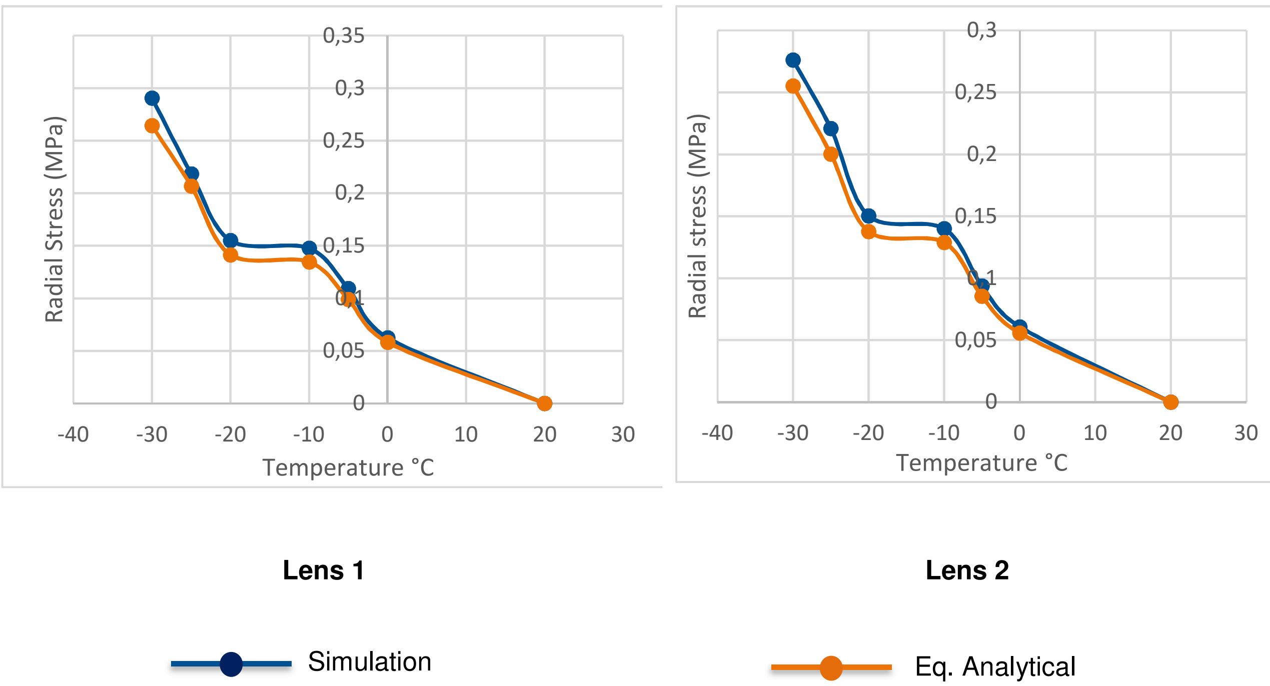

Fig. 6. Radial stress curve as a function of the temperature

DOI: 10.13009/EUCASS2023-324

Table 8. Values of errors between simulated and analytical method for each element lenses for different temperatures

Glasses	Temperature (°C)						
	20°C	0°C	-5°C	-10°C	-20°C	-25°C	-30°C
Lens 1	0	7.795	7.810	7.630	8.210	8.604	9.852
Lens 2	0	4.465	7.874	8.207	5.538	8.930	9.550

It can be seen from Fig.6, that the absolute value of the radial stress of the lens gradually increase with the decrease of the temperature for both lenses for simulation. The values are very small and close to zero. Under the same conditions, use the analytical equations analyzed and derived in the previous section to find the analytical solution of the radial stress, which is presented errors in Table.8, the difference observed between the simulation and those obtained from analytical method are the same order for both lenses. They are most often less than 10%, which is acceptable.

6. conclusion

This paper proposes a new study on the thermal effects of athermal bonding thickness, thermal stress, radial stress, and thermal optical path difference based on existing research. The proposed model is validated using finite element analysis.

The use of a six-point edge bond is shown to generally produce lower thermal stress levels than a continuous bond, and it can also be athermalized. Additionally, the Deluzio, Muench, Van Bezooijen, and Monti equations (2-5) can be used for most athermal optimum bondline calculations. For lens assembling, an analytical method is established for cases where thermal stress is low and adverse for both lenses. This is achieved by considering the presence of a mechanical temperature gradient parameter. The thermal stress is proportional to the thermal distortion coefficient for space applications.

The use of a face bond produces low radial stresses, resulting in thermal bonding of the optical surface and a lower risk of structure failure. However, the allowable stress is the failure stress associated with some probability of failure at a given lifetime. This condition must be checked for optical effects by using the optical path difference (OPD) and compared to the admissible optic. The effects of temperature variations on the OPD can be directly imported into a variety of optical analyses to predict performance due to thermal loads.

When performing less distortion and aiming for a quarter wavelength tolerance for diffraction-limited performance on the lens, the Rayleigh criterion can be applied. Comparing the detailed finite-element results to analytical solutions for simplified models provides good estimates of radial stress. However, it should be noted that the accuracy of any analytical or finite element results is only as good as the material constants used in the analysis. Finally, the error is found to be within 10%, which allows for an improvement in accuracy over cost, subject to proper approximation. This finding is particularly relevant in the context of space structure calculations.

7. Reference

1. Fishers, R.E., 1991. Case study of elastomeric lens mounts. Optomechanics and dimensional stability. IN: Proc. Of SPIE Vol. 1533, PP.27-35.
2. Hagyong. K., Yang, Hu-Soon., Lee, Yun-woo., 2011. Athermal lens mount with ring flexures. Journal of the Korean physical society, Vol. 59, No.6, PP.3356-3362.

DOI: 10.13009/EUCASS2023-324

3. Bayar, M., 1981. Lens barrel optomechanical design principles. Optical Engineering, 20 (2), 202181.
4. Vukobratovich, D., Bonded mounts for small cryogenic optics, SPIE Vol .4131.
5. Yoder, P., 2002. Mounting optics in optical instruments. SPIE press P.72
6. Deluzio, A.J., 1968. Optimization of elastomer thickness for edge mounted mirrors subject to uniform temperature changes. Itek, technical report ATR 68-16.
7. Vukobratovich, D., Yoder, P., 2018. Fundamentals of optomechanics optical sciences and applications of light. CRC press Taylor& Francis Group LLC.
8. Monti, C.L., 2007., Athermal bonded mounts incorporating aspect ratio into a closed form solution, Proc. SPIE, 6665-666503.
9. Vukobratovich, D., July 1992. Rugged yet light weight: how can we achieve both in optical instruments. Critical review Vol.CR43, optomechanical design, ed.P.R.Yoder, Jr. copyright SPIE.
10. Herbet, J., 2006. Techniques for deriving optimal bondlines for athermal bonded mounts, current developments in lens design and optical engineering VII, Proc of SPIE Vol, 6288, 62880J. doi: 10.1117/12.680828.
11. Anees, A., 2017. Handbook of optomechanical engineering, second edition. CRC press Taylor & Francis Group
12. Sparks, M., Cottis, M., 1973. Pressure induced optical distortion in laser windows, J. Appl. Phys., 44, 787.
13. Yoder, P. R. Jr., 2008. Mounting optics in optical instruments. Second edition, SPIE, copyright © society of photo-optical instrumentation engineers.
14. Yoder, P. R. Jr., Vukobratovich, D, 2015. Opto-mechanical systems design. Volume 1, fourth edition. Design and analysis of opto-mechanical assemblies, CRC press is an imprint of Taylor & Francis Group.
15. Hsu, M-Y., Chang, S-T., Huang, T-M, 2012. Thermal optical path difference analysis of the telescope correct lens assembly. Adv. Opt. Techn.., 1(6): 447-453.
16. Keith, B.D, 2002. Athermal design of nearly incompressible bonds. proceedings of SPIE-The international society for optical engineering. 4771:296-303. Doi: 10.117/12.482171.
17. Maamar, F., Boudjemai, A. 2020. Opto-mechanical optimal design configuration and analysis of glue pad bonds in lens mounting for space application, Advances in space research, 0273-1177© COSPAR published by Elsevier Ltd. Doi: 10-1016/j.asr.2020.01.025.
18. Weinswing, S., Hookman, R.A., Dec 1991. Optical analysis of thermal induced structural distortions, Proc of SPIE. Vol.1527, current developments in optical design and optical engineering, ed. R. E. Fischer, W.J. smith. Copyright SPIE.
19. Vyacheslav, M. R. 2007. Analysis of thermal stress and deformation in elastically bonded optics. New developments in optomechanics, edited by Alson E. Hatheway, proc of SPIE Vol. 6665, 66650K. Doi: 10.1117/12.732217.
20. Jamieson, T.H. 1981. Thermal effects in optical systems. Optical engineering. Vol 20, N°02. 156-160.